Journal of Chromatography A, 1219 (2012) 161–172

Contents lists available at SciVerse ScienceDirect

Journal of Chromatography A

journal homepage: www.elsevier.com/locate/chroma

Effect of varying flow regimes upon elution behaviour, apparent molecular characteristics and hydrodynamic properties of amylopectin isolated from normal corn starch using asymmetrical flow field-flow fractionation

Shazia Juna*, Anton Huber[1]

NAWI Graz-CePol/MC (Molecular Characteristics), Institute for Chemistry, University of Graz, Heinrichstrasse 28, 8010 Graz, Austria[2]

ARTICLE INFO

Article history:
Received 22 August 2011
Received in revised form 9 November 2011
Accepted 12 November 2011
Available online 19 November 2011

Keywords:
Amylopectin
Asymmetrical flow field-flow fractionation
High pressure microwave vessel
Molar mass
Retention

ABSTRACT

A detailed study of the elution behaviour, apparent molecular characteristics and hydrodynamic properties of amylopectin-type fraction (isolated from normal corn starch) in aqueous media employing asymmetrical flow field-flow fractionation (AF4) was undertaken by systematically varying the channel flow (F_{ch}), cross flow (F_{cr}) and F_{cr}/F_{ch} ratios. Distributions of apparent molar masses and radii of gyration, mass recoveries and hydrodynamic radii decreased as a function of increasing F_{cr} at a fixed F_{ch}, due to the increase in the retention of amylopectin-type fraction in the AF4 channel. Increased retention of the amylopectin-type fraction in the AF4 channel was also observed at low F_{ch} and high F_{cr}/F_{ch} ratios. Large amylopectin-type molecules/particles (possibly aggregates) eluted at high F_{ch}, low F_{cr} and low F_{cr}/F_{ch} ratios.

1. Introduction

Asymmetrical flow field-flow fractionation (AF4) has been employed for the separation of dispersed or completely solubilised colloids and macromolecules in aqueous media [1–7]. AF4 coupled with multi-angle light scattering and a refractive index detector (AF4/MALS/RI) has become a well-established technique for the determination of average values and distributions of molar mass and radii of gyration for native starches and modified starches [3,8–17].

1.1. Asymmetrical flow field-flow fractionation (AF4)

The separation of molecules/particles in AF4 is governed by differences in their translational diffusion co-efficients (D_T) [6–8]. The D_T (Eq. (1)) and hydrodynamic radii (R_h) (Eq. (2)) values of molecules and particles can be determined from AF4 parameters and retention time (t_r) assuming a spherical geometry [7],

$$D_T = \frac{t^0 F_{cr} w^2}{6V^0} \frac{1}{t_r} \quad (1)$$

$$R_h = \frac{k_B T V^0}{\pi \eta t^0 F_{cr} w^2} t_r \quad (2)$$

t^0 is the void time, F_{cr} is the cross flow rate, w is the channel thickness, V^0 is the geometric void volume, t_r is the retention time, k_B is Boltzmann's constant, T is the absolute temperature and η is the viscosity coefficient of the solvent.

The retention parameter, λ, is related to AF4 parameters and the D_T of the molecule/particle (Eq. (3)) [7].

$$\lambda = \frac{DV^0}{F_{cr} w^2} \quad (3)$$

1.2. Molecular characteristics of starches determined using AF4/MALS/RI

Starch occurs in the form of granules, which have varying degrees of structural order, and consists of two major polysaccharides: amylose and amylopectin [18–21]. Amylose consists predominantly of linear α(1→4)-linked glucopyranose chains with some branching (10 branch points per molecule). Amylopectin also contains sequences of α-(1→4)-linked glucopyranose units, although it also has extensive branching via α-(1→6)-linked glucopyranose units [18–21]. The molar mass (M_w) of amylose reported in the literature ranges from 10^5 g/mol to 10^6 g/mol while that for amylopectin ranges from 10^7 g/mol to 10^8 g/mol [10,15–19]. Detailed surveys of the variety of dissolution procedures, including the use of high pressure microwave vessel (HPMV)

* Corresponding author. Tel.: +43 3163805435; fax: +43 3163809850.
E-mail address: shazia.juna@uni-graz.at (S. Juna).
[1] Member of EPNOE.
[2] Partner of EPNOE – European Polysaccharide Network of Excellence.

0021-9673/$ – see front matter © 2011 Elsevier B.V. All rights reserved.
doi:10.1016/j.chroma.2011.11.024

Table 1
Overview of molar masses (M_w), radii of gyration (R_g) and hydrodynamic radii (R_h) values of various amylopectin sources determined using asymmetrical flow field-flow fractionation coupled with multi-angle light scattering and a refractive index detector reported in the literature.

Flow regimes/strategy	Material and dissolution method	M_w (10^{-6} g/mol)	R_g (nm)	R_h (nm)	Refs.
F_{cr} rates (0.1–0.3 mL/min), fixed F_{ch} rate	Waxy barley in H_2O autoclaved at 121 °C for 20 min	156–216	197–270	–	[12]
F_{cr}/F_{ch} = 0.24 mL/min (fixed), various F_{cr} and F_{ch} rates	Waxy corn in H_2O autoclaved at 120 °C, 20 min	–	250–450	80–300	[9]
Fixed F_{ch} rate of 1.0 mL/min, exp. decay F_{cr} rates (0.4–0 mL/min)	Amylopectin (8 varieties) in H_2O, 40 s HPMV treatment	105–318	163–229	–	[11]
Non-linear F_{cr} programme	Waxy corn in H_2O, high pressure cell treatment at 140 °C, 10 min	492	–	–	[13]
Fixed F_{ch} rate of 1.0 mL/min, exp. decay F_{cr} rates (1.0–0 mL/min)	Waxy corn and waxy rice in H_2O, autoclaved at 150 °C, 40 min.	390	230–240	24–550	[14]
Fixed F_{ch} rate of 1.0 mL/min, F_{cr} rates (1.0–0.1 mL/min) systematic linear variation & non-linear F_{cr} programming	Waxy corn in 1 M KSCN, 60 s HPMV treatment	27–33	135–146	28–178	[10]
Fixed F_{ch} rate of 1.0 mL/min, F_{cr} rates (1.0–0.1 mL/min) systematic linear variation	Amylopectin fractions (3 varieties) in 1 M KSCN, HPMV treatment 60 s	17–62	73–140	10–252	[15–17]

Table 2
Average apparent molar mass ($M_{w,app}$) and apparent radius of gyration ($R_{g,app}$) values determined for amylopectin-type fraction (normal corn starch) with varied cross flow rates (F_{cr}) and varied channel flow rates (F_{ch}) at fixed F_{cr}/F_{ch} ratios.

F_{ch} (mL/min)	F_{cr} (mL/min)	LS detectors included	$M_{w,app}$ (g/mol)	$R_{g,app}$ (nm)	R_h (nm)	% mass recovery
Fixed F_{cr}/F_{ch} ratio of 0.3						
1.0	0.3	26°, 35°, 43°, 52°, 60°, 69°, 80°, 90°, 100°, 111°, 121°, 132°, 142°, 153°, 163°	37×10^6	129	21–140	86
0.7	0.2	80°, 90°, 100°, 111°, 121°, 132°, 142°, 153°, 163°	37×10^6	144	41–191	42
0.35	0.1	35°, 43°, 52°, 60°, 69°, 80°, 90°, 100°, 111°, 121°, 132°, 142°, 153°, 163°	10×10^6	131	35–120	38
Fixed F_{cr}/F_{ch} ratio of 1.0						
1.0	1.0	26°, 35°, 43°, 52°, 60°, 69°, 80°, 90°, 100°, 111°, 121°, 132°, 142°, 153°, 163°	10×10^6	134	10–70	42
0.7	0.7	26°, 35°, 43°, 52°, 60°, 69°, 80°, 90°, 100°, 111°, 121°, 132°, 142°, 153°, 163°	9×10^6	146	28–90	25
0.5	0.5	35°, 43°, 52°, 60°, 69°, 80°, 90°, 100°, 111°, 121°, 132°, 142°, 153°, 163°	4×10^6	127	32–129	26
0.35	0.35	26°, 35°, 43°, 52°, 60°, 69°, 80°, 90°, 100°, 111°, 121°, 132°, 142°, 153°, 163°	1.3×10^6	79	21–60	17

treatment for dissolving starch materials [9–11,15–17,22,23], have previously been discussed [10,15–17]. Considerable variations in the literature values of molar masses and sizes for starch-glucans (including amylopectin) arise due to the differences in botanical origin, dissolution methods and analytical techniques employed [10,15–17,20–30].

M_w and R_g values reported in the literature for waxy corn (99% amylopectin) range from 19.5×10^6 g/mol [31] to 4092×10^6 g/mol [13] and 62 nm [32] to 372 nm [33], respectively. Similarly, literature values for M_w and R_g for amylopectin isolated from normal corn starch range from 10×10^6 g/mol [22] to 490×10^6 g/mol [33] and 94 nm [15] to 259 nm [27], respectively. These variations in the literature values illustrate the variations in molecular characteristics of amylopectin arising from the differences in samples, isolation procedures, dissolution methods and analytical techniques employed [10,15–17,21,24].

The separation and characterisation of amylopectin materials employing AF4/MALS/RI has been reported by a number of researchers, as shown in Table 1. Variation in the literature values of M_w and sizes of amylopectin (waxy starches and isolated fractions from native starches) occur due to differences in the samples, dissolution procedures and, possibly, AF4 flow regimes. Average M_w and R_g values of amylopectin samples dissolved in water by heating either by autoclaving at temperatures ~150 °C [13,14] are considerably higher than M_w and R_g values determined for amylopectin heated in HPMV for 40 s [11]. Lower apparent average molar mass ($M_{w,app}$) and apparent average radii of gyration ($R_{g,app}$) for amylopectin materials dissolved in 0.035 M KSCN by heating in a HPMV for 60 s have been reported [10,15–17]. These variations in the molar masses and sizes may be due to the differences in the sources of the amylopectin samples and the dissolution processes employed.

A variety of flow regimes employed for the separation and characterisation of amylopectin have been reported in the literature (Table 1). Wahlund et al. [14], Bowen et al. [13], and Rolland-Sabate et al. [11] employed non-linear cross-flow programming (F_{cr} decrease exponentially at a fixed F_{ch}). Rolland-Sabate et al. employed a fixed F_{ch} of 1.0 mL/min and F_{cr} were exponentially reduced from 0.4 mL/min to 0 mL/min for the initial 400 s then no F_{cr} was applied for the remainder of the elution time [11]. The researchers reported that amylopectin did not elute at high F_{cr} rates, indicating the presence of ultra-high molecular weight material. Wahlund et al. employed a similar exponential decay programme where, at a fixed F_{ch} of 1.0 mL/min, the F_{cr} was exponentially reduced from 1.0 mL/min to 0 mL/min for 20 min and reported the elution of amylopectin at low F_{cr} [14]. Juna et al. examined both linear and non-linear programming for the separation of waxy corn starch and showed that the retention of amylopectin molecules increased as a function of increasing F_{cr} [10]. The influence of varying F_{cr} at a fixed F_{ch} of 1.0 mL/min for amylopectin-type fractions isolated from normal corn [15], native sago [17] and native tapioca [16] starches upon their elution behaviour and apparent molecular characteristics were previously reported. Van Bruijnsvoort et al. investigated the effect of varying both F_{cr} and F_{ch} at a fixed F_{cr}/F_{ch} ratio of 0.24 on the retention behaviour of amylopectin and reported a decrease in the apparent R_h and R_g values as a function of increasing F_{ch} and F_{cr} [8].

Although light scattering provides absolute values for the molar masses and sizes for macromolecules, due to the high sensitivity of starch-glucan materials to dissolution protocols, separation

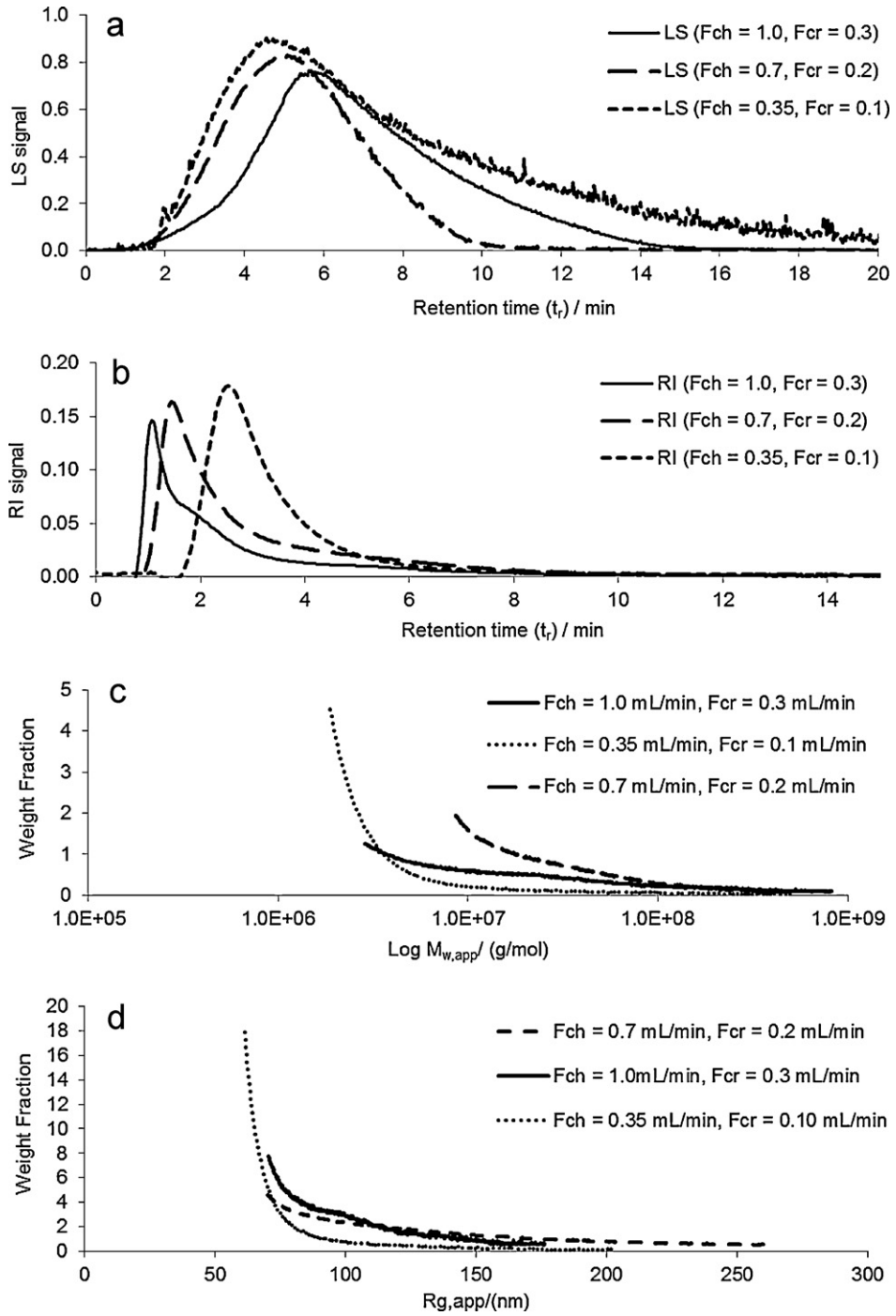

Fig. 1. Fixed F_{cr}/F_{ch} ratio of 0.3 with various combinations of F_{ch} and F_{cr}: (a) LS (90°) versus retention time; (b) RI versus retention time; (c) differential $M_{w,app}$ distributions and (d) differential $R_{g,app}$ distributions.

methods and their inherent nature (botanical origins, sample sources) the molar masses and radii of gyration reported in this publication are reported as apparent rather than absolute values to reflect the complexity of starch-glucan materials. Aggregation of the starch molecules in aqueous media is a dynamic process which occurs to varying degrees depending on dissolution procedure and the inherent nature of the sample. AF4 is a suitable technique for the investigation of these large aggregates by studying their retention behaviour, molecular characteristics and hydrodynamic properties. The aim of this publication is to present a detailed account of the effects of varying F_{ch}, F_{cr} and F_{cr}/F_{ch} ratios on the elution behaviour of amylopectin fractions isolated from native normal corn starch dissolved in 0.035 M KSCN in a high pressure microwave vessel.

2. Materials and methods

Amylopectin-type fraction was isolated from a commercial sample of normal corn starch (National Starch) via selective precipitation method as reported by Greenwood and Banks with minor modifications [34].

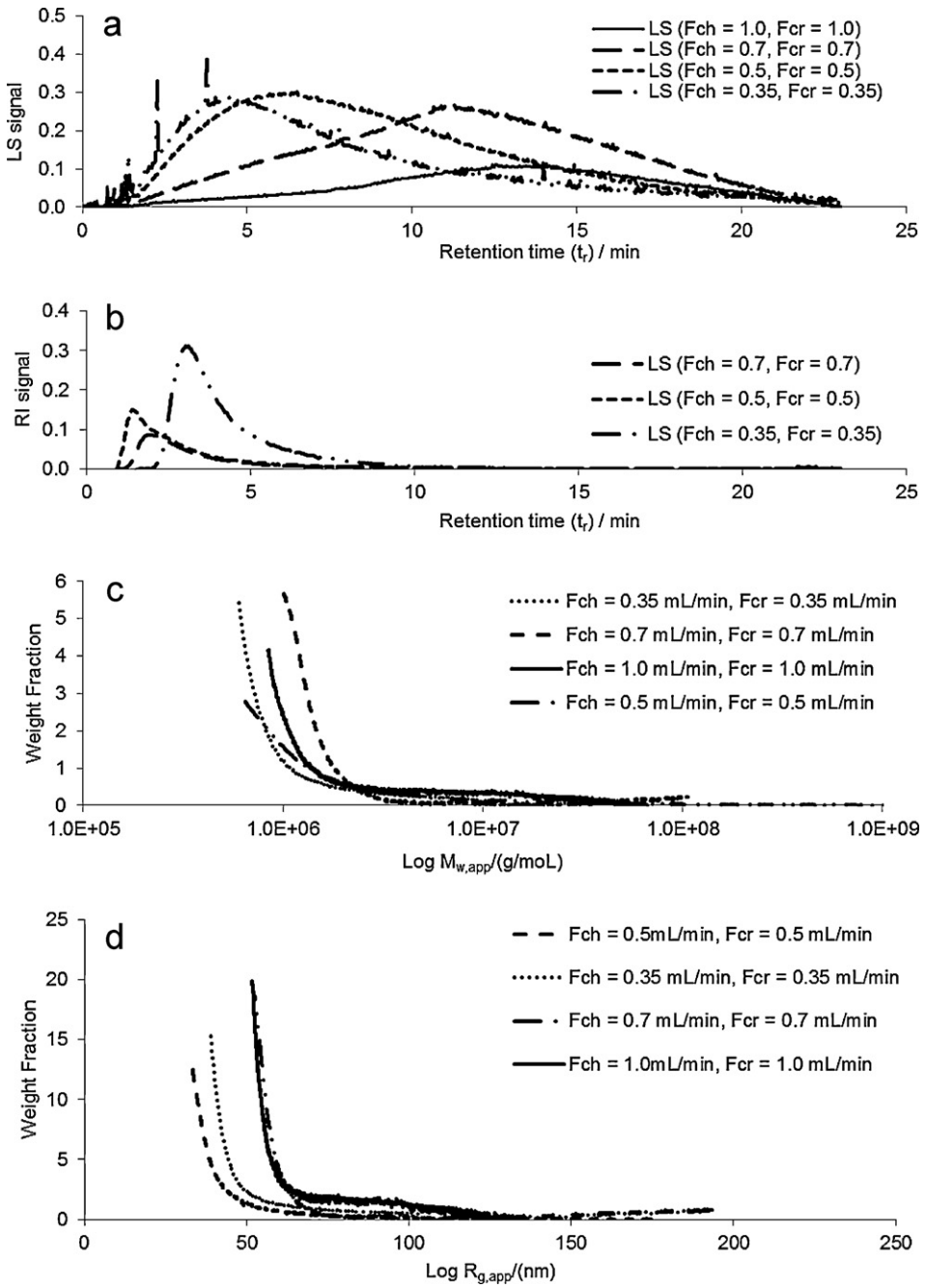

Fig. 2. Fixed F_{cr}/F_{ch} ratio of 1.0 with various combinations of F_{ch} and F_{cr}: (a) LS (90°) versus retention time; (b) RI versus retention time; (c) differential $M_{w,app}$ distributions and (d) differential $R_{g,app}$ distributions.

2.1. Determination of amylose content in amylopectin-type fraction

The amount of amylose in the isolated amylopectin-type fraction was determined using a UV/VIS spectrophotometer (Ocean Optics; USB4000 Fibre Optic Spectrometer, DH-2000-BAL Deuterium/halogen light source) at a wavelength of 630 nm. A series of standard solutions with known amylose and amylopectin content were used to obtain a calibration curve. The absorbance of I_2-amylose complex in amylopectin-type fraction was measured and the amylose content was found to be 0.05% determined from the calibration curve. This method has been outlined by Séne et al. [35].

2.2. Dissolution of amylopectin-type in aqueous media

An amylopectin-type fraction isolated from normal corn starch was dissolved in 0.035 M KSCN by heating in a high pressure microwave vessel (HPMV) for 60 s, was previously reported [10,15–17]. Aqueous solution of amylopectin-type fraction (concentrations of 0.14 mg/mL) was prepared as follows: 20–30 mg of amylopectin-type fraction (normal corn) was left to stir at 18 °C in 50 mL of 1 M KSCN for 12 h. 20 mL of the solution was then transferred into the Teflon cup of a HPMV (total volume 45 mL, Polycarbonate model 4782, Parr Instrument Co., Moline, IL) and heated in a microwave oven (90% power, 800 W) for 60 s. The stock solutions were cooled in an ice bath for 1 h, then diluted with deionised

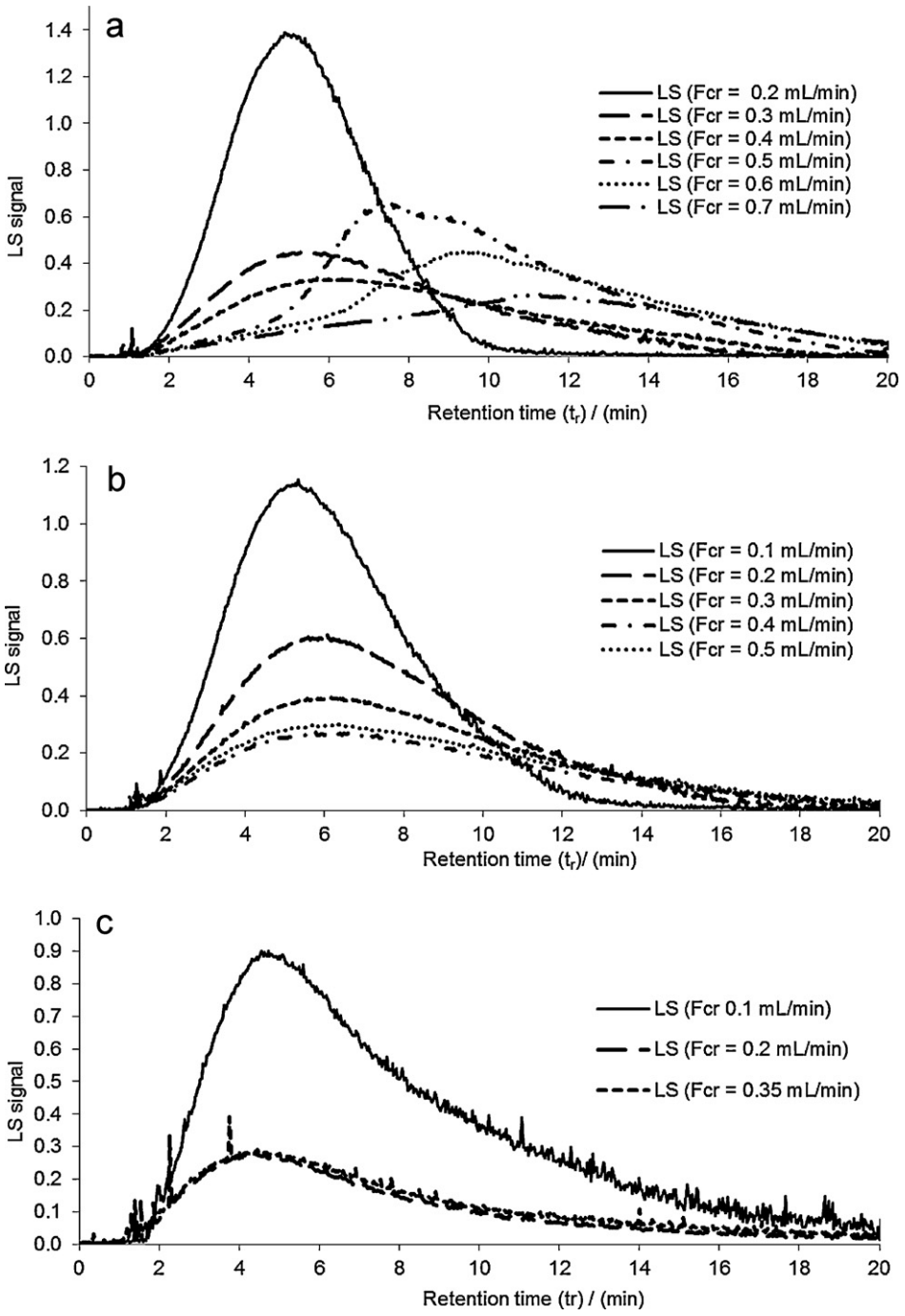

Fig. 3. The effect of varying cross flow rates (F_{cr}) upon the LS profiles for amylopectin-fraction (normal corn starch) obtained at a fixed channel flow rate (F_{ch}) of (a) 0.7 mL/min, (b) 0.5 mL/min and (c) 0.35 mL/min.

water to yield starch samples dissolved in 0.035 M KSCN. The d*n*/d*c* value of 0.151 for amylopectin-type fraction dissolved in 0.035 M KSCN was determined experimentally.

2.3. Determination of molecular characteristics using AF4/MALS/RI

The AF4 set-up (ConSenxus, Ober-Hilbersheim, Germany) employed consisted of: a vacuum degasser (Cambridge Scientific Instruments Ltd., Ely, UK); a 0.22 μm inline filter (Millipore (U.K.) Ltd., Watford, UK); a Flow Box P 2.1 (ConSenxus, Ober-Hilbersheim, Germany); a Savebox V5 (ConSenxus, Ober-Hilbersheim, Germany); an AF4 channel (comprising an impermeable upper channel wall and a permeable lower accumulation channel wall, dimensions: 320 mm × 100 mm × 145 mm and with an accumulation wall area 36.09 cm^2, polysulphone membrane (M_w-cut-off of 10 kDa), a 190 μm spacer and a 100 μL injector sample loop); detection units (multi-angle laser light scattering Wyatt Dawn® EOS (λ = 690 nm) with toluene-based calibration constant of 9.04×10^{-6}; mass detector (Wyatt Optilab DSP) at 632 nm with a NaCl-based calibration constant of 2.369×10^{-5}); ASTRA for Windows 4.90 (Wyatt Technology Corporation, Germany) managed by ConSenxus WinFFF Control V. 4.0 software. The AF4 channel thickness (w) was found to be 165 μm from Bovine Serum Albumin (known D_T value of 5.96×10^{-7} cm^2/s at 294 K) measurements.

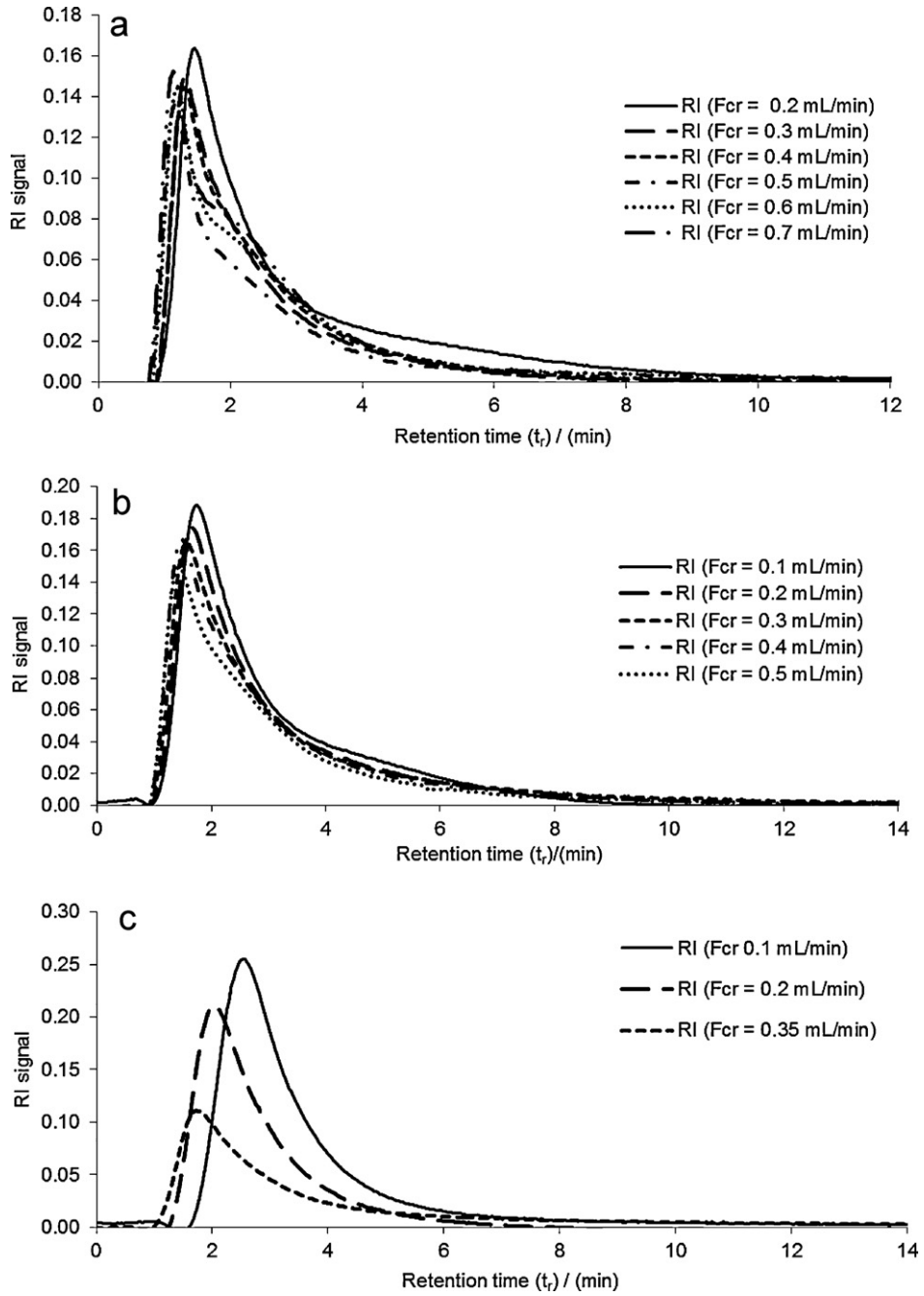

Fig. 4. The effect of varying cross flow rates (F_{cr}) upon the RI profiles for amylopectin-fraction (normal corn starch) obtained at a fixed channel flow rate (F_{ch}) of (a) 0.7 mL/min, (b) 0.5 mL/min and (c) 0.35 mL/min.

Starch solutions were analysed on a AF4-MALS/RI setup by injecting 100 μL of each sample solution with degassed 0.035 M KSCN, containing 0.05% NaN_3, filtered through a Millipore 0.2 μm cellulose nitrate filter, as eluent. The optimum focusing period of 7 min (determined by direct observation of amylopectin-azure solution) at a F_{ch} of 2.5 mL/min and a F_{cr} of 2.4 mL/min. Scattering intensities at λ = 690 nm were recorded at 18 scattering angles (θ) ranging between 26° and 143°. Molar mass (M_w) is determined from the intercept of the $c \to 0$ and $\theta \to 0$ double extrapolation, while R_g is obtained from the slope of the $\theta \to 0$ extrapolation (Eq. (4)) [5,8,10,11].

$$\sqrt{\frac{Kc}{R_\theta}} = \sqrt{\frac{1}{M_w} + \frac{16\pi^2}{3\lambda^2} {R_g}^2 \sin^2\left(\frac{\theta}{2}\right)} \quad (4)$$

M_w represents the weight-average molar mass, R_θ is the excess Rayleigh factor, K is an optical and instrumental constant and λ is the laser wavelength.

3. Results and discussion

3.1. Elution behaviour of amylopectin-type fraction (normal corn starch) at fixed F_{cr}/F_{ch} ratios

The effect of F_{cr}/F_{ch} ratios on the elution behaviour of amylopectin-type fraction was investigated by selecting a range of F_{cr} and F_{ch} to yield F_{cr}/F_{ch} ratios of 0.3 (low) and 1.0 (high). The initial spike (~1–1.8 min) observed in the refractive index (RI) peaks (Fig. 1b) is an experimental artefact which corresponds to the pressure variation arising during the transition from

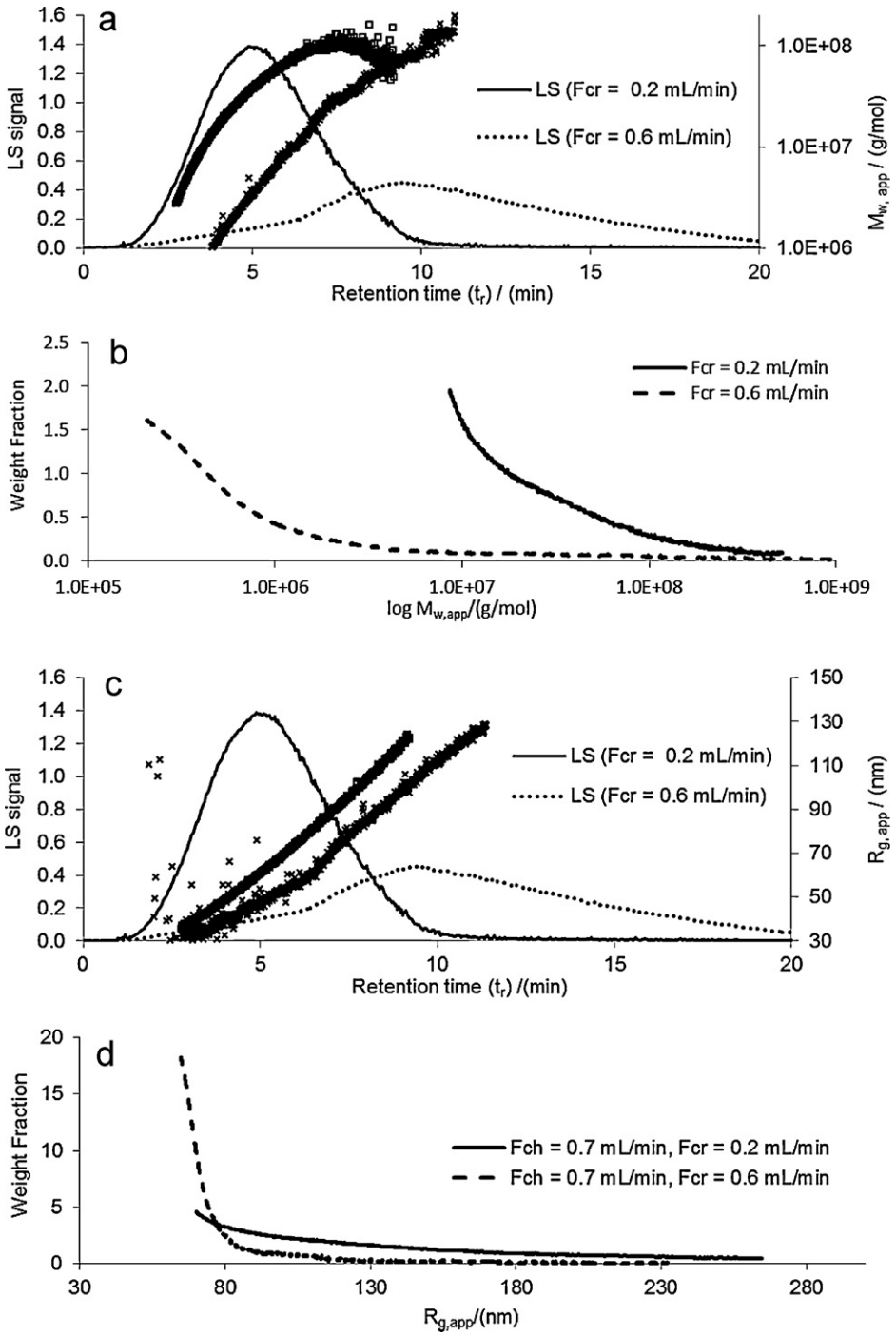

Fig. 5. The effect of varying cross flow rates (F_{cr}) at a fixed channel flow rate of 0.7 mL/min upon: (a) Apparent molar mass ($M_{w,app}$) as a function of retention time (t_r) with superimposed LS peaks; (b) differential $M_{w,app}$ distributions; (c) Apparent radii of gyration ($R_{g,app}$) as a function of retention time (t_r) with superimposed LS peaks; (d) differential $R_{g,app}$ distributions for amylopectin-type fraction.

focusing to elution. As light scattering (LS) peaks (Fig. 1a) begin from ~2 min, the RI data corresponding to the experimental artefact were excluded from data processing. The LS peaks obtained at a fixed F_{cr}/F_{ch} ratio of 0.3 mL/min are very broad (~2 min to >10 min) while the corresponding RI peaks indicate that the majority of the amylopectin fraction eluted within the initial 8 min. In the presence of lower F_{ch} the amylopectin-type fraction eluted later, as observed from the RI peaks (Fig. 1b), and the corresponding mass recoveries also decreased (Table 2). While at high F_{cr}, the mass recoveries increased, which is contrary to our previous findings where the mass recoveries decreased as a function of increasing F_{cr} obtained at a fixed F_{ch} of 1.0 mL/min [15]. This suggests that both F_{ch} and F_{cr}, even at a fixed F_{cr}/F_{ch} ratio, influence the retention behaviour of amylopectin-type fraction. The LS intensities did not change significantly with varying F_{ch} and F_{cr} (Fig. 1a). However, broadening of LS peaks was observed in the presence

of high F_{ch} of 1.0 mL/min and 0.7 mL/min. An average apparent molar mass ($M_{w,app}$) value of 37×10^6 g/mol for amylopectin-type fraction was obtained with high F_{ch} (1.0 mL/min and 0.7 mL/min), while at a low F_{ch} of 0.35 mL/min a considerably lower average $M_{w,app}$ value of 10×10^6 g/mol was determined (Table 2). The corresponding differential $M_{w,app}$ distributions (Fig. 1c) for amylopectin-type fraction obtained at a low F_{ch} of 0.35 mL/min shows that the majority of the eluted amylopectin-type consists of macromolecules under 10×10^6 g/mol, while at high F_{ch} higher differential $M_{w,app}$ distributions ranging from $\sim 10^7$ g/mol to over 10^8 g/mol were obtained for amylopectin-type fraction. At high F_{cr}, the amylopectin-type fraction was increasingly retained, which can be seen from the differential $M_{w,app}$ distributions (Fig. 1c). The average $R_{g,app}$ values for amylopectin-type fractions did not appear to change as a result of variations in F_{cr} or F_{ch} (Table 2). The differential $R_{g,app}$ distributions for amylopectin-type fraction (Fig. 1d) indicate that at low F_{ch} of 0.35 mL/min, the majority of the material consists of comparatively smaller (~70 nm) molecules/particles compared to high F_{ch} (1.0 mL/min and 0.7 mL/min) where the majority of the amylopectin-type molecules/particles sizes range from ~75 nm to ~100 nm. The presence of large amylopectin-type macromolecules/particles, $R_{g,app}$ values ranged from ~100 nm to ~150 nm, was observed at high F_{ch}. R_h values for amylopectin-type fraction determined using Eq. (4), ranged from ~20 nm to ~191 nm, and were unaffected by variations in F_{cr} and F_{ch} at a fixed F_{cr}/F_{ch} ratio of 0.3 (Table 2). In contrast, Van Bruijnsvoort et al. reported that at a fixed F_{cr}/F_{ch} ratio of 0.24, apparent R_h and R_g values decreased as a function of increasing F_{ch} and F_{cr} in the presence of steric-hyperlayer mode of separation [8]. We observed a normal mode of separation, as both $M_{w,app}$ and $R_{g,app}$ for amylopectin-type fraction increased as a function of retention time (Fig. 5a and c). The differences in the behaviour of amylopectin between this investigation and that of Van Bruijnsvoort et al. [8] are therefore due to the variations in the dissolution protocols and source of amylopectin samples.

At a higher fixed F_{cr}/F_{ch} ratio of 1.0, the majority of the amylopectin-type fraction eluted within 8 min (Fig. 2b), as was previously observed at a fixed F_{cr}/F_{ch} ratio of 0.3 (Fig. 1b). Broadening of LS peaks and lower LS intensities were observed as a function of increasing F_{ch} and F_{cr} (Fig. 2a). The average $M_{w,app}$ values, average $R_{g,app}$ values and mass recoveries for amylopectin-type increased as a function of increasing F_{ch} and F_{cr} (Table 3). The differential $M_{w,app}$ distributions obtained for amylopectin-type fraction were very similar for all F_{cr} and F_{ch} at a fixed F_{cr}/F_{ch} ratio of 1.0 (Fig. 2c). The differential $M_{w,app}$ distributions show that the majority of the amylopectin-type material eluted at a high F_{cr}/F_{ch} ratio of 1.0, with $M_{w,app}$ ranging from $\sim 1 \times 10^6$ g/mol to $\sim 5 \times 10^6$ g/mol, while molecules/particles with ultra-high $M_{w,app}$ were retained in the AF4 channel (Fig. 2c). The differential $M_{w,app}$ distributions and corresponding mass recoveries for amylopectin-type obtained at a high F_{cr}/F_{ch} ratio of 1.0 were considerably lower than the ones obtained at a low F_{cr}/F_{ch} ratio of 0.3. This behaviour indicates that the retention of amylopectin-type fraction in the AF4 channel increased at a very high F_{cr}/F_{ch} ratio of 1.0. At low F_{ch} (0.35 mL/min and 0.5 mL/min), the majority of the amylopectin-type fraction eluted consisted of smaller macromolecules ($R_{g,app}$ ~40–50 nm), as seen from the differential $R_{g,app}$ distributions for amylopectin-type fraction (Fig. 2d). At high F_{ch} (0.7 mL/min and 1.0 mL/min), the majority of the amylopectin-type fraction eluted consisted of slightly larger molecules/particles ($R_{g,app}$ ~65 nm), and in the case of F_{ch} of 1.0 mL/min, the presence of very large molecules/particles (~70–100 nm) was also observed (Fig. 2d). At high F_{cr}/F_{ch} ratio of 1.0, compared to low F_{cr}/F_{ch} ratio of 0.3, an increased retention of large molecules/particles occurred in the AF4 channel; this in turn resulted in the lower apparent molecular characteristics and hydrodynamic size of amylopectin-type fraction. This study demonstrates that the retention of amylopectin-type materials is greatly influenced by both F_{cr} and F_{ch}, even when the F_{cr}/F_{ch} ratio was fixed.

3.2. The effect of varying F_{cr} at a fixed F_{ch}

We have previously demonstrated that at a fixed F_{ch} of 1.0 mL/min, the mass recoveries, R_h and apparent molar masses of amylopectin-type fraction decrease as a function of increasing F_{cr}, which was attributed to the increase in the retention of amylopectin-type molecules/particles in the AF4 channel [10,15]. The influence of varying F_{cr} for a range of fixed F_{ch} of 0.7 mL/min, 0.5 mL/min and 0.35 mL/min was undertaken to investigate the influence of F_{cr} on the elution behaviour of amylopectin-type fraction (normal corn). F_{cr} were typically varied from 0.1 mL/min to an upper-limit of F_{cr} equal to the F_{ch} in regular increments of 0.1 mL/min. The majority of the amylopectin-type fraction eluted within the initial ~8 min for all F_{ch} and F_{cr}, as seen from the RI profiles (Fig. 4). The mass recoveries obtained for amylopectin-type fraction decreased as a function of increasing F_{cr} for all fixed F_{ch} (Table 3), indicating that amylopectin-type fraction is increasingly retained in the AF4 channel in the presence of high F_{cr}. Broadening of LS peaks and a decrease in LS intensities as a function of increasing F_{cr} (Fig. 3) was observed for all fixed F_{ch}, which also indicates that large molecules/particles were retained in the AF4 channel at high F_{cr}. Average $M_{w,app}$ average $R_{g,app}$ and R_h values decreased as a function of increasing F_{cr} for all fixed F_{ch} (Table 3). The differential $M_{w,app}$ distribution obtained for amylopectin-type fraction at a fixed F_{ch} of 0.7 mL/min and a F_{cr} of 0.6 mL/min, indicates that the majority of the material eluted with $M_{w,app}$ ranging from $\sim 3 \times 10^5$ g/mol to $\sim 5 \times 10^6$ g/mol, while the population of the molecules/particles exceeding 10×10^6 g/mol is very small (Fig. 5b). In contrast, higher differential $M_{w,app}$ distributions were observed for amylopectin-type fraction at a fixed F_{ch} of 0.7 mL/min and a F_{cr} of 0.2 mL/min, indicating that majority of the amylopectin-type material eluted consisted of molecules/particles with very high $M_{w,app}$ ranging from 10×10^6 g/mol to 100×10^6 g/mol. The presence of exceedingly large amylopectin-type molecules/particles with $M_{w,app}$ values ranging from 100×10^6 g/mol to $\sim 1000 \times 10^6$ g/mol was observed at a low F_{cr} of 0.2 mL/min but not for the high F_{cr} of 0.6 mL/min (Fig. 5b). Similarly, a decrease in the differential $R_{g,app}$ distributions was also observed as a function of increasing F_{cr} (Fig. 5d). At a high F_{cr} of 0.6 mL/min, the majority of the amylopectin-type material eluted ranged from ~70 nm to ~85 nm while at a low F_{cr} of 0.2 mL/min the majority of the material eluted ranged from ~70 nm to ~250 nm. The decrease in the differential $M_{w,app}$ distributions, differential $R_{g,app}$ distributions, R_h and mass recoveries for amylopectin-type fraction as a function of increasing F_{cr} suggest that very large molecules/particles were increasingly retained in the AF4 channel (Fig. 5a and c; Table 3).

D_T and R_h ranges were determined from retention time (t_r) and AF4 parameters (Eq. (4)), assuming a spherical conformation for amylopectin-type fraction (Fig. 4). High D_T values for amylopectin-type fraction ranging from $\sim 2 \times 10^{-7}$ cm^2/s to $\sim 3 \times 10^{-8}$ cm^2/s were obtained at high F_{cr} of 0.5–0.7 mL/min at a fixed F_{ch} of 0.7 mL/min (Fig. 6a). A corresponding decrease in the R_h values for amylopectin-type fraction as a function of increasing F_{cr} was also observed for all fixed F_{ch} investigated (Fig. 6b). Lower λ values (Fig. 6c) were obtained at very high F_{cr} (0.6–0.7 mL/min), which suggest that molecules/particles are gradually pushed towards the accumulation wall and, therefore, increasing the retention of the amylopectin material as well as increasing the sample-membrane interactions.

Table 3
Average apparent molar mass ($M_{w,app}$) and apparent radius of gyration ($R_{g,app}$) values obtained for amylopectin-type fraction (normal corn starch) obtained with varying cross flow rates (F_{cr}) and fixed channel flow rates (F_{ch}).

F_{cr} (mL/min)	LS detectors included	$M_{w,app}$ (g/mol)	$R_{g,app}$ (nm)	R_h (nm)	% mass recovery
Fixed F_{ch} (0.7 mL/min)					
0.2	80°, 90°, 100°, 111°, 121°, 132°, 142°, 153°, 163°	37×10^6	144	41–191	42
0.3	60°, 69°, 80°, 90°, 100°, 111°, 121°, 132°, 142°, 153°, 163°	22×10^6	125	28–156	41
0.4	60°, 69°, 80°, 90°, 100°, 111°, 121°, 132°, 142°, 153°, 163°	19×10^6	108	28–144	38
0.5	35°, 43°, 52°, 60°, 69°, 80°, 90°, 100°, 111°, 121°, 132°, 142°, 153°, 163°	17×10^6	130	27–126	36
0.6	35°, 43°, 52°, 60°, 69°, 80°, 90°, 100°, 111°, 121°, 132°, 142°, 153°, 163°	13×10^6	179	30–108	34
0.7	26°, 35°, 43°, 52°, 60°, 69°, 80°, 90°, 100°, 111°, 121°, 132°, 142°, 153°, 163°	9×10^6	146	28–90	25
Fixed F_{ch} (0.5 mL/min)					
0.1	35°, 43°, 52°, 60°, 69°, 80°, 90°, 100°, 111°, 121°, 132°, 142°, 153°, 163°	24×10^6	137	115–252	51
0.2	35°, 43°, 52°, 60°, 69°, 80°, 90°, 100°, 111°, 121°, 132°, 142°, 153°, 163°	16×10^6	124	79–168	38
0.3	35°, 43°, 52°, 60°, 69°, 80°, 90°, 100°, 111°, 121°, 132°, 142°, 153°, 163°	11×10^6	122	60–156	34
0.4	35°, 43°, 52°, 60°, 69°, 80°, 90°, 100°, 111°, 121°, 132°, 142°, 153°, 163°	6×10^6	126	36–149	31
0.5	35°, 43°, 52°, 60°, 69°, 80°, 90°, 100°, 111°, 121°, 132°, 142°, 153°, 163°	4×10^6	127	32–129	26
Fixed F_{ch} (0.35 mL/min)					
0.1	35°, 43°, 52°, 60°, 69°, 80°, 90°, 100°, 111°, 121°, 132°, 142°, 153°, 163°	10×10^6	131	35–120	38
0.2	26°, 35°, 43°, 52°, 60°, 69°, 80°, 90°, 100°, 111°, 121°, 132°, 142°, 153°, 163°	6×10^6	126	25–72	27
0.35	26°, 35°, 43°, 52°, 60°, 69°, 80°, 90°, 100°, 111°, 121°, 132°, 142°, 153°, 163°	1.3×10^6	79	21–60	17

3.3. Effect of increasing F_{ch} at fixed F_{cr} on the elution behaviour of amylopectin-type (normal corn)

At a fixed F_{cr} of 0.5 mL/min, the F_{ch} were varied from 0.5 mL/min to 1.0 mL/min, to investigate the effect of varying F_{ch} on the elution behaviour and molecular characteristics of amylopectin-type fraction. Broadening of LS peaks and increase in the LS intensities were observed as a function of decreasing F_{ch} (Fig. 7a). As discussed previously (Section 3.1), the initial RI data corresponding to ~1 min to ~2 min were excluded from data processing as these were experimental artefacts. Broadening of the RI peaks (Fig. 7b) and decrease in the mass recoveries (Table 4) were observed as a function of increasing F_{ch}. The average $M_{w,app}$ values decreased as a function of increasing F_{cr}, while average $R_{g,app}$ values remained consistent (Table 4). At a fixed F_{cr} of 0.5 mL/min and for all F_{ch}, the differential $M_{w,app}$ distributions indicate that the majority of

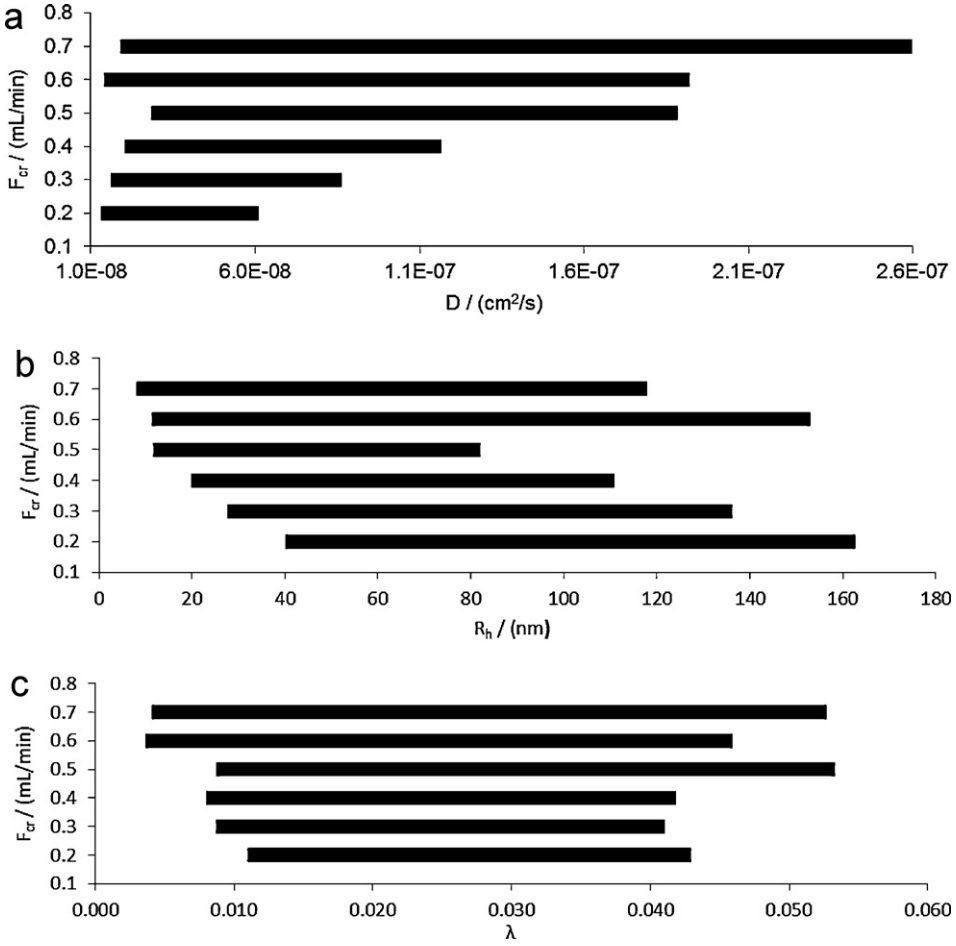

Fig. 6. Effect of varying cross flow rates (F_{cr}) (0.2 mL/min to 0.7 mL/min) at a fixed channel flow rate (F_{ch}) of 0.7 mL/min obtained for amylopectin-type (corn) upon (a) translational diffusion co-efficients (D_T); (b) hydrodynamic radii (R_h) values and (c) retention parameter (λ).

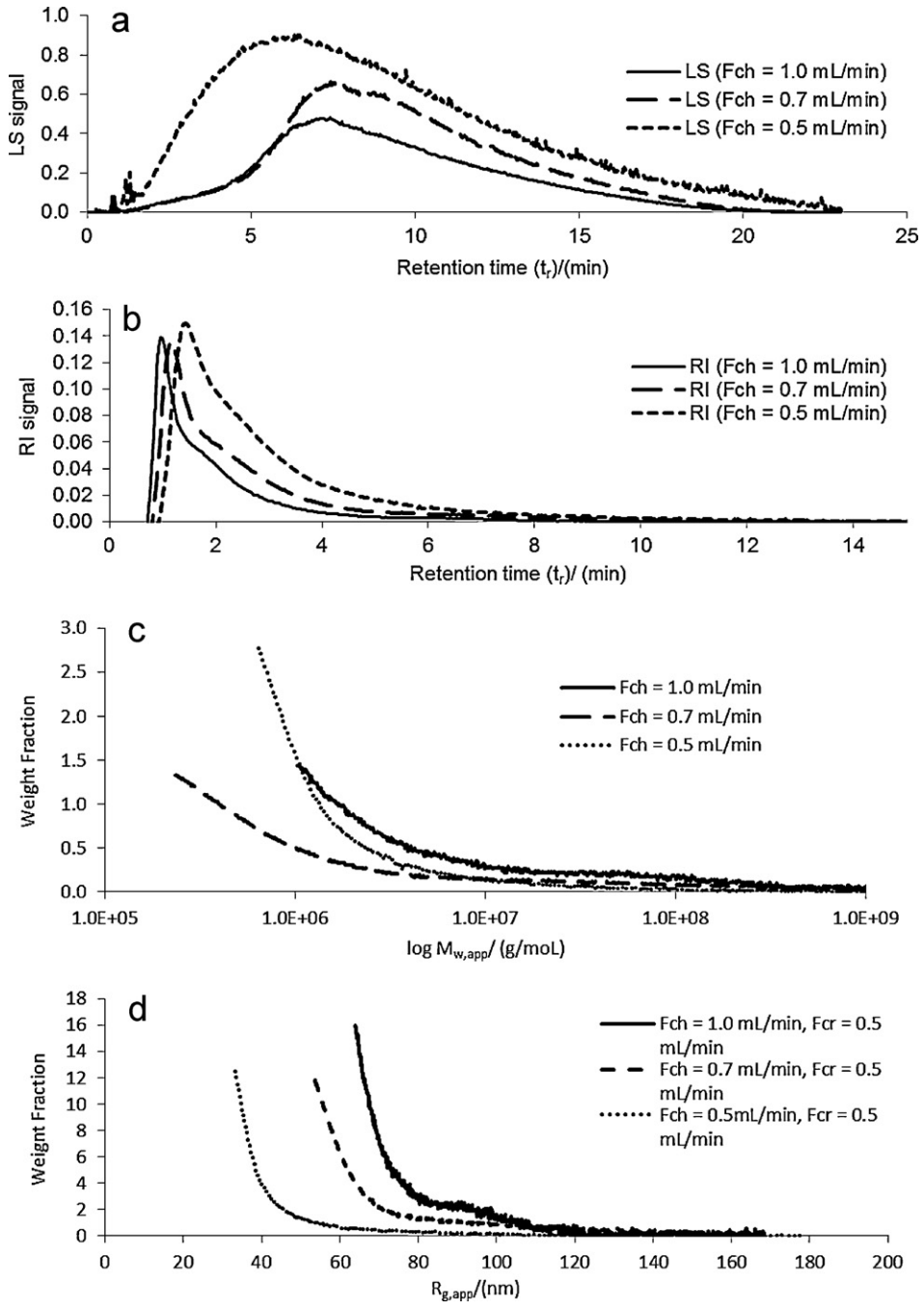

Fig. 7. The effect of varying channel flow rates (F_{ch}) at a fixed cross flow rate (F_{cr}) of 0.5 mL/min for amylopectin-type (normal corn) on (a) LS (90°) signals; (b) RI peaks; (c) differential $M_{w,app}$ distributions and (d) differential $R_{g,app}$ distributions.

Table 4
Average apparent molar mass ($M_{w,app}$) and apparent radius of gyration ($R_{g,app}$) values determined for amylopectin-type fraction (normal corn starch) with varying channel flow rates (F_{ch}) at a fixed cross flow rate (F_{cr}) of 0.5 mL/min.

F_{ch} (mL/min)	LS detectors included	$M_{w,app}$ (g/mol)	$R_{g,app}$ (nm)	R_h (nm)	% mass recovery
1.0	26°, 35°, 43°, 52°, 60°, 69°, 80°, 90°, 100°, 111°, 121°, 132°, 142°, 153°, 163°	40×10^6	115	14–112	74
0.7	35°, 43°, 52°, 60°, 69°, 80°, 90°, 100°, 111°, 121°, 132°, 142°, 153°, 163°	17×10^6	130	27–126	36
0.5	35°, 43°, 52°, 60°, 69°, 80°, 90°, 100°, 111°, 121°, 132°, 142°, 153°, 163°	4×10^6	127	32–129	26

the amylopectin-type fraction consisted of molecules/particles with $M_{w,app}$ values ranging from $\sim 1 \times 10^6$ g/mol to 5×10^6 g/mol (Fig. 7c). However, molecules/particles with ultra-high $M_{w,app}$ values ranging from $\sim 10 \times 10^6$ g/mol to over 100×10^6 g/mol were observed at a high F_{ch} of 1.0 mL/min. The differential $R_{g,app}$ distributions indicate that the majority of amylopectin-type material eluted consisted of compact and small molecules/particles (~35–50 nm) at a low F_{ch} of 0.5 mL/min while at a high F_{ch} of

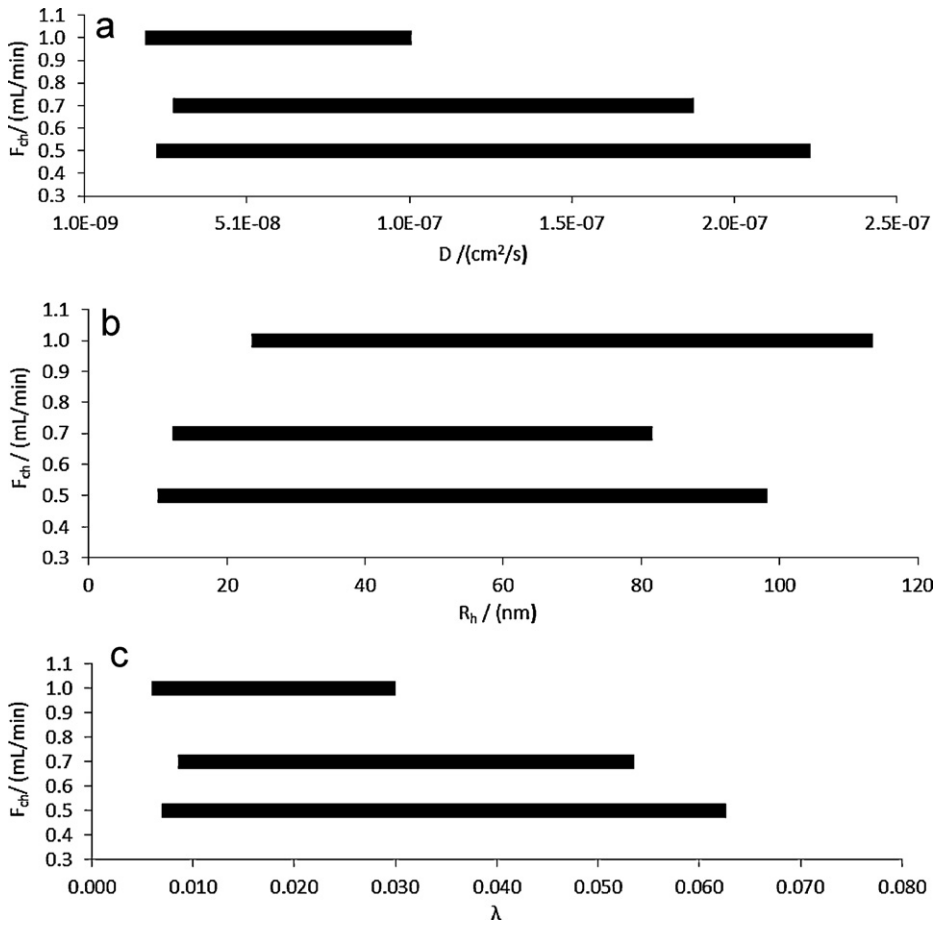

Fig. 8. Effect of varying channel flow rates (F_{ch}) (1.0 mL/min to 0.5 mL/min) at a fixed cross flow rate (F_{cr}) of 0.5 mL/min obtained for amylopectin-type (corn) upon (a) translational diffusion co-efficients (D_T); (b) hydrodynamic radii (R_h) values; (c) retention parameter (λ).

1.0 mL/min most of the material ranged from ~65 nm to over 100 nm (Fig. 7d).

At low F_{ch} (0.5 mL/min and 0.7 mL/min) high D_T values were obtained, indicating the elution of small amylopectin-type molecules/particles (corresponding R_h values range from ~15 nm to ~80 nm). While at a high F_{ch} of 1.0 mL/min the amylopectin-type molecules/particles with low D_T values corresponding to R_h values ranging from ~25 nm to ~115 nm (Fig. 8) Low retention parameter (λ) values were obtained for high F_{ch}, which indicate that the large amylopectin-type molecules were positioned closer to the accumulation wall, and that the approximate concentration zone (thickness of the layer) of these larger molecules in the AF4 channel was very low. As amylopectin-type molecules/particles elute more rapidly at high F_{ch} from the AF4 channel, the analyte zone also diminishes rapidly. At low F_{ch}, the amylopectin-type material resides longer in the AF4 channel and elutes gradually in comparison with high F_{ch}, increasing the interactions between the amylopectin-type molecules/particles as well as sample-membrane interactions.

4. Conclusion

The retention behaviour of amylopectin-type fraction (isolated from normal corn starch) dissolved in 0.035 M KSCN was investigated by undertaking a detailed study of the variation of mass recoveries, apparent molecular characteristics and hydrodynamic properties by systematically varying F_{cr}, F_{ch} and F_{cr}/F_{ch} ratios. Low differential $M_{w,app}$ distributions and differential $R_{g,app}$ distributions of amylopectin-type were obtained with high F_{cr}, low F_{ch} and high F_{cr}/F_{ch} ratio. Increased retention of amylopectin-type fraction in the AF4 channel was observed at high F_{cr}, resulting in the decrease in mass recoveries, apparent molecular characteristics and R_h values for amylopectin-type glucans (normal corn). F_{ch} controls the speed of molecules/particles during elution, therefore, an increase in both inter- and intra-molecular interactions of amylopectin-type molecules/particles as well as an increase in sample-membrane interactions are anticipated at low F_{ch}. High D_T values were obtained at low F_{ch}, indicating the elution of small and compact amylopectin-type molecules/particles while large molecules/particles remained longer in the AF4 channel. Low retention parameter (λ) values determined at high F_{cr} at a fixed F_{ch} indicate that the amylopectin-type molecules were pushed closer towards the membrane. While, at a fixed F_{cr} of 0.5 mL/min and with high F_{ch} the low λ values indicate that amylopectin-type molecules/particles eluted rapidly from the AF4 channel, as the analyte zone diminished rapidly.

The apparent molecular characteristics and hydrodynamic properties of amylopectin-type fraction, dissolved in 0.035 M KSCN, were influenced by variations in the AF4 flow regimes resulting in variations in their retention behaviours. While the elution behaviour, apparent molecular characteristics and hydrodynamic properties of amylopectin-type sample (starch-glucans in general) determined with a single flow regime provides some information regarding their retention behaviour, by investigating the apparent molecular characteristics, hydrodynamic properties obtained across a range of flow conditions, an overall pattern in the retention behaviour of the material can be observed. This comprehensive approach may be employed to investigate the influence of other dissolution protocols for amylopectin or starch-glucan

materials as a means to investigate the nature of such materials and possible degrees of aggregation arising from various dissolution procedures.

References

[1] F.A. Messaud, R.D. Sanderson, J.R. Runyon, T. Ote, H. Pasch, S.K.R. Williams, Prog. Polym. Sci. 34 (2009) 351.
[2] G. Yohannes, M. Jussila, K. Hartonen, M.-L. Riekkola, J. Chromatogr. A 1218 (2011) 4104.
[3] S. Lee, S.T. Kim, B.R. Pant, H.D. Kwen, H.H. Song, S.K. Lee, S.V. Nehete, J. Chromatogr. A 1217 (2010) 4623.
[4] S. Lee, P.-O. Nilsson, G.S. Nilsson, K.-G. Wahlund, J. Chromatogr. A 1011 (2003) 111.
[5] B. Wittgren, K.-G. Wahlund, J. Chromatogr. A 760 (1997) 205.
[6] G. Modig, L. Nilsson, B. Bergenståhl, K.-G. Wahlund, Food Hydrocolloids 20 (2006) 1087.
[7] K.-G. Wahlund, in: M. Schimpf, K. Caldwell, J.C. Giddings (Eds.), Field Flow Fractionation Handbook, Wiley-Interscience, New York, 2000, p. 279.
[8] M. van Bruijnsvoort, K.-G. Wahlund, G. Nilsson, W.Th. Kok, J. Chromatogr. A 925 (2001) 171.
[9] A. Rolland-Sabaté, T. Sánchez, A. Buléon, P. Colonna, B. Jaillais, H. Ceballos, Food Hydrocolloids 27 (2012) 161.
[10] S. Juna, S. Davies, P.A. Williams, Carbohydr. Polym. 83 (2011) 1384.
[11] A. Rolland-Sabaté, P. Colonna, M.G. Mendez-Montealvo, V. Planchot, Biomacromolecules 8 (2007) 2520.
[12] S. You, M.S. Izodorczyk, K.R. Preston, Cereal Chem. 79 (2002) 624.
[13] S. Bowen, D.A. Gray, C. Giraud, M. Majzoobi, C.E.M. Testa, L.A. Bello-Perez, S.E. Hill, J. Cereal Sci. 43 (2006) 275.
[14] K.-G. Wahlund, M. Leeman, Anal. Bioanal. Chem. 399 (2011) 1455.
[15] S. Juna, A. Huber, Starch, in press.
[16] S. Juna, A. Huber, Starch, in press.
[17] S. Juna, A. Huber, Starch, in press.
[18] L.A. Bello-Perez, S.L. Rodriguez-Ambriz, M.M. Sanchez-Rivera, E. Agama-Acevedo, in: A. Bertolini (Ed.), Starches: Characterization, Properties, and Applications, Taylor & Francis, Boca Raton, 2010, p. 33.
[19] S. Perez, P.M. Baldwin, D.J. Gallant, in: R. Whistler, J. BeMiller (Eds.), Starch Chemistry and Technology, 3rd ed., Elsevier Inc., London, 2009, p. 149.
[20] P. Taggart, in: G. Phillips, P.A. Williams (Eds.), Handbook of Hydrocolloids, 2nd ed., CRC, Boca Raton, 2009, p. 108.
[21] M.J. Gidley, I. Hanashiro, N.M. Hani, S.E. Hill, A. Huber, J.-L. Jane, Q. Liu, G.A. Morris, A. Rolland-Sabaté, A.M. Striegel, Carbohydr. Polym. 79 (2010) 255.
[22] L. Belloperez, P. Roger, B. Baud, P. Colonna, J. Cereal Sci. 27 (1998) 267.
[23] A. Rolland-Sabate, A.N. Georges, D. Dufour, S. Guilois, P. Colonna, J. Sci. Food Agric. 83 (2003) 927.
[24] R.A. Cave, S.A. Seabrook, M.J. Gidley, R.G. Gilbert, Biomacromolecules 10 (2009) 2245.
[25] Y.–L. Chung, H.-M. Lai, Carbohydr. Polym. 63 (2006) 527.
[26] J.-A. Han, H. Lim, S.-T. Lim, Starch – Stärke 57 (2005) 262.
[27] J. Han, Carbohydr. Polym. 55 (2004) 193.
[28] J.H. Lee, J.–A. Han, S.-T. Lim, Food Hydrocolloids 23 (2009) 1935.
[29] W. Praznik, A. Huber, J. Chromatogr. B 824 (2005) 295.
[30] L. Bello-Pérez, P. Colonna, P. Roger, O. Parees-Lopez, Carbohydr. Polym. 37 (1998) 383.
[31] M.L. Fishman, P.D. Hoagland, Carbohydr. Polym. 23 (1994) 175.
[32] L. Elfstrand, T. Frigård, A. Roger, A.-C. Eliasson, M. Jönsson, M. Wahlgren, Carbohydr. Polym. 57 (2004) 389.
[33] S.H. Yoo, J.-L. Jane, Carbohydr. Polym. 49 (2002) 307.
[34] F. Ahmad, P.A. Williams, J.-L. Doublier, S. Durand, A. Buléon, Carbohydr. Polym. 38 (1999) 361.
[35] M. Séne, C. Thévenot, J.L. Prioul, J. Cereal Sci. 26 (1997) 21.